Published in final edited form as:
Anal Chem. 2012 June 19; 84(12): 5250–5256. doi:10.1021/ac300128p.

Asynchronous magnetic bead rotation (AMBR) micro-viscometer for rapid, sensitive and label-free studies of bacterial growth and drug sensitivity

Irene Sinn[1,2,3], **Theodore Albertson**[1,4], **Paivo Kinnunen**[1,5], **David N. Breslauer**[6], **Brandon H. McNaughton**[1,2,5], **Mark A. Burns**[3], and **Raoul Kopelman**[1,2,4,5,*]

[1]Department of Chemistry, University of Michigan, 930 North University, Ann Arbor, MI 48109-1055

[2]Department of Biomedical Engineering, University of Michigan, 2200 Bonisteel, Ann Arbor, MI 48109-2099

[3]Department of Chemical Engineering, University of Michigan, 2300 Hayward Street, Ann Arbor, MI 48109-2136

[4]Department of Physics, University of Michigan, 450 Church Street, Ann Arbor, MI 48109-1040

[5]Applied Physics Program, University of Michigan, 2477 Randall Laboratory, Ann Arbor, MI 48109-1120

[6]Refactored Materials, Inc, San Francisco, CA 94158-2509

Abstract

The long turnaround time in antimicrobial susceptibility testing (AST) endangers patients and encourages the administration of wide spectrum antibiotics, thus resulting in alarming increases of multi-drug resistant pathogens. A method for faster detection of bacterial proliferation presents one avenue towards addressing this global concern. We report on a label-free asynchronous magnetic bead rotation (AMBR) based viscometry method that rapidly detects bacterial growth and determines drug sensitivity by measuring changes in the suspension's viscosity. With this platform, we observed the growth of a uropathogenic *Escherichia coli* isolate, with an initial concentration of 50 cells per drop, within 20 minutes; in addition, we determined the gentamicin minimum inhibitory concentration (MIC) of the *E. coli* isolate within 100 minutes. We thus demonstrated a label-free, micro-viscometer platform that can measure bacterial growth and drug susceptibility more rapidly, with lower initial bacterial counts than existing commercial systems, and potentially with any microbial strains.

1. Introduction

Early diagnosis of microbial infections helps patients and helps address the global problem of the emergence and spread of antimicrobial resistance.[1–3] The current 'gold standard' for clinical antimicrobial susceptibility testing (AST) is a growth-based broth microdilution technique used to determine the minimum inhibitory concentration (MIC). The broth microdilution MIC is defined as the lowest antibiotic concentration that inhibits visible microbial growth after overnight incubation. In contrast to the traditional methods that require overnight incubation, modern and automated techniques can provide results in 6–24

*Phone: (734) 764-7541, Fax: (734) 936-2778, kopelman@umich.edu.

Supporting Information Available: This material is available free of charge via the Internet at http://pubs.acs.org

hours, after the initial incubation and enrichment process. These long testing times lead to patients being prescribed empiric, wide spectrum therapies, which can result in poor patient response and, moreover, contribute to increases in multi-drug resistant pathogens.[4] As a result, there is a need for an AST method that can provide results within hours rather than days, enabling patients to be treated more rapidly and with more appropriate therapies,[5] while minimizing increases in drug resistant populations.[4,6–8] The ongoing goal of the authors is to develop an ultra-rapid technology that expedites and refines the use of antibiotics for patients with life-threatening bacterial infections, including outbreaks due to newly emerged antibiotic resistant strains. Nucleic acid tests (NAT), which detect resistant genes, are increasingly used as adjuncts for AST;[9] however, NAT lacks the ability to determine antibiotic MIC, differentiate mutant strains, or identify resistance of species, where resistance is expressed through many mechanisms (e.g. gram-negative bacteria).[7,8] As a result, phenotypic growth-based assays remain the gold standard for AST.[10,11]

Commercial automated phenotypic AST systems commonly use the *colorimetric turbidity-based broth microdilution technique* to measure bacterial proliferation. These AST systems require an initial bacteria count of at least 10^5 bacteria per antibiotic sample, i.e. test well, and take 6–24 hours to determine the MIC value; this still does not take into account the initial bacterial enrichment and isolation stage, which typically takes over 24 hours. There have been recent advancements towards reducing the detection time, by measuring bacterial metabolism,[12] by elongation and division of a single or small population of bacteria,[13,14] and by increasing the effective bacterial concentrations through confinement into smaller volumes.[2,12,14,15] Although these techniques can detect proliferation and determine susceptibility within hours, they often rely on microscopy (e.g. fluorescence microscopy) or specific-antibody based techniques.

Measuring environmental (e.g. change in viscosity) changes due to bacterial proliferation offers a versatile technique for measuring microbial growth without relying on antibodies or complex detection systems.[16–19] Bacteria in a planktonic state exhibit unique hydrodynamic and rheological properties that depend on bacterial species, concentration, and health.[20] For instance, directional motility of planktonic bacteria affects solution viscosity; specifically, contractile bacteria increase solution viscosity and extensile bacteria reduces solution viscosity.[17,19–22] The bacterial concentration and availability of oxygen and nutrients also affect solution viscosity through their effect on bacterial motility and polysaccharides secretion.[23–25] For example, a high concentration of bacteria in a suspension, such as biofilm-forming of quorum-sensing bacteria, secrete polysaccharides that are typically higher in molecular weight and more viscous;[26] these polysaccharides change the solution's rheology from Newtonian to viscoelastic and non-Newtonian.[23] It has also been reported that the viscosity of a broth solution decreases upon proliferation, as bacteria ingest the large, viscous macromolecules within the broth.[16,18,27] Despite the variety of mechanisms that cause viscosity changes, our experiments, as described below, illustrate that bacterial proliferation alters the hydrodynamic and rheological properties of a suspension.

Here we report on an asynchronous magnetic bead rotation (AMBR) droplet microfluidic micro-viscometer that detects bacterial proliferation by measuring changes in the suspension's rheological properties. The AMBR sensor is a recently reported device that is based on monitoring the time-dependent *asynchronous* rotation of a magnetic bead that is within an external rotating magnetic field.[13,14,28–34] This sensor monitors the magnetic and physical properties of the magnetic bead and the environmental viscosity in which the bead resides.[13,14,29–35] Notably, only in the asynchronous regime can such parameters, including viscosity, be measured continuously by the magnetorotation frequency.[13,14,28–34] We apply this sensitive AMBR micro-viscometer towards rapid AST applications. The approach reported herein is a significant advancement over our previously reported antibody-based

AST system as the AMBR micro-viscometry is a novel, label-free approach for measuring microbial growth and AST.[14] As a result, the AMBR micro-viscometer is a versatile platform that can be used with any bacterial strain. Other methods to measure viscosity at small volumes include viscosity sensitive dyes, microacoustic sensors, cantilevers and depolarization fluorescence spectroscopy.[36–38] However, in contrast to the reported AMBR micro-viscometer here, these systems typically require larger volumes, chemical or physical labeling, and/or expensive or complex equipment. The individual AMBR viscometers are encapsulated in microfluidic water-in-oil (w/o) nanoliter droplets,[14] AST may be performed with an initial bacterial count of 50, or fewer, cells per droplet. With AMBR micro-viscometry, we successfully determined the gentamicin MIC of a uropathogenic *Escherichia coli* isolate within 100 minutes. Therefore, we have demonstrated a label-free, AMBR micro-viscometer platform that can be used to perform rapid AST applications on any microbial strain. Furthermore, to perform AST, this platform requires 1000-fold fewer bacteria than commercial systems; this may further reduce the overall AST time, i.e. reduce the sample prep and enrichment time. This new system, as a tool that significantly reduces AST time, has the potential to help patients get prompt and focused drug treatment, as well as to combat the global threat of antimicrobial resistance.

2. Experimental Section

2.1 Reagents

PCR grade mineral oil and bovine serum albumin (BSA) were purchased from Sigma-Aldrich Corp. ABIL® EM 90 was graciously donated by Evonik Goldschmidt GmbH. Mueller Hinton II (MH Broth) was purchased from Teknova. Dispensing and inlet/outlet adaptors were purchased from Nordson, EFD and Small Parts Inc., respectively. Pluronic F-68 was purchased from MP Biochemicals. 16 ± 2 μm carboxyl superparamagnetic particles and the 8.8 ± 0.8 μm carboxyl-, amino-, and streptavidin-functionalized magnetic particles were purchased from Spherotech, Inc. 10 μm NIST traceable size standards were purchased from Polysciences, Inc. Glycerol was purchased from Fisher Sci. The continuous phase consisted of mineral oil with 3 % ABIL® EM 90 (w/w). The aqueous phase consisted of MH broth with 1% Pluronic F-68 and 0.1 % BSA, which will be referred to as MH-PB.

2.2 Device Fabrication

The fabrication process on a glass wafer is detailed elsewhere.[14,39] Briefly, 50 nm Cr and 250 nm Au were evaporated onto the wafer. After patterning, the microfluidic channels were etched with hydrofluoric acid to a depth of 40 – 45 μm, as measured with a surface profilometer. The metal layers were removed, devices diced, and inlets/outlet electrochemically drilled. The devices were cleaned in Piranha solution and subsequently coated with a 2 μm parylene layer. The devices were UV-glued to a standard cover glass slide, thickness No. 2 (Electron Microscopy Sciences), and the inlet and outlet ports (Small Parts, Inc.) were UV-glued to the device. The schematic and assembled microfluidic droplet device is shown in Figure 1(a). All used devices were recovered and re-used. Device recovery entails separating the glass device from the cover glass and inlet/outlet ports with methanol and heating devices to 410 °C for 2 hours. Used devices were cleaned in Piranha solution and the process above was repeated.

2.3 Magnetic Janus particle fabrication

The fabrication procedure for Janus particles is detailed elsewhere.[40,41] Briefly, 500 μL of 16 μm carboxyl magnetic particles (1% w/v) (Spherotech) were spin-coated onto a 4″ glass wafer. A 50 nm layer of Al was evaporated onto the surface. The particles were recovered and suspended in PBS. The resultant Janus particles, which will be referred to as magnetic Janus particles, enabled better visualization of the particle's rotation (following the

"MagMOON" principle)[28,41, 42] at lowered magnification, enabling multiple AMBR sensors to be monitored concurrently. Non-specific binding was not observed, and the Al coating was not observed to affect bacterial cell growth.

Magnetically uniform Janus particles were fabricated using the process detailed above, with modifications. Rather, 300 nm of Ni was evaporated onto the 10 μm NIST polystyrene particles (Polysciences), the wafer was magnetized in a 60 mT permanent magnetic field for 3 days and the particles were recovered. The resultant Janus particles will be referred to as magnetically uniform Janus particles.

2.4 Particle Characterizations on non-specific binding

10 μL of each of the 8.8 μm carboxyl-, amino-, and streptavidin-functionalized magnetic particles (Spherotech) were added to 1 mL of a 1×10^7 CFU/mL solution. The particles and bacteria were incubated at 37 °C on a shaking platform for 2 hours. After incubation, 10 μL of the solution was visualized with light microscopy to determine the degree of non-specific binding.

2.5 Experimental Procedure

The microfluidic device was flushed with Rain-X® Original Glass Treatment (SOPUS Products) for 5 minutes to increase surface hydrophobicity.[14] The continuous phase and 15 μL of aqueous phase were introduced to their respective inlet reservoir. 1 nL w/o droplets were formed by adjusting the vacuum strength and hydrostatic pressure of the outlet and oil phase, respectively.

For characterization experiments, the aqueous phase consisted of MH-PB and the magnetically uniform Janus particles. For growth experiments, an MH-PB solution was inoculated with a clinical uropathogenic *E. coli* isolate to a 0.5 McFarland standard (~ 1.5×10^8 CFU/mL), and subsequently diluted to achieve approximately 50 bacteria per droplet. Bacterial growth and AST were performed on a microfluidic device platform (Fig. 1a,b), in which individual AMBR biosensors were encapsulated into nanoliter volume droplets (Fig. 1c). As bacteria in their planktonic state grow and divide in the surrounding solution (Fig. 1d), the viscosity of the AMBR complex changes, which is detected by a measurable shift in the bead's rotational frequency (Fig. 1e). Antibiotic response experiments were conducted serially for the present system; the bacteria inoculated into a gentamicin solution, with final gentamicin concentrations of 0, 0.25, 0.5, 1, and 2 μg/mL. Experiments started within 30 minutes of antibiotic exposure.

The description of the experimental set-up is detailed elsewhere.[14] Briefly, the temperature was maintained at 37 ± 0.2 °C using a temperature-controlled ITO slide. This system was placed inside custom-built electromagnet coils, and the rotating magnetic field was generated with a custom LabView program. The magnetic field strength at the region of interest, e.g. droplet chamber, was measured to be 0.71 ± 0.03 mT, and the driving frequency was set at 200 Hz for experiments using magnetically uniform Janus particles. For growth experiments, the magnetic field strength at the region of interest was set at 2.4 ± 0.4 mT, with a driving frequency of 10 Hz.

For the growth experiments, continuous videos at 10 frames per second (fps) were taken over at least 3 hours. Videos of the rotating magnetic bead were analyzed with ImageJ and MATLAB. Briefly, the light intensity at a region of interest on the magnetic bead is monitored for at least 10 bead rotation cycles using ImageJ, generating a quasi-sinusoidal signal that corresponds with each rotation. The Fourier transform of the raw quasi-sinusoidal signal is a custom MATLAB program and the bead's rotational frequency is calculated [Supplementary Fig. 1]. Each experimental run was conducted in triplicates; i.e. at least

three droplets, each droplet enclosed an individual magnetic bead, were monitored per experimental condition. The illustrated experimental error in the rotational period is the full width half max (FWHM) of the Fourier transform of the raw rotational signal, or equal to the standard deviation of measurement, where appropriate, of the representative runs.[28]

3. Results and Discussion

3.1 Concept of the Asynchronous Magnetic Bead Rotation (AMBR) Viscometer

The theory behind the AMBR biosensor is detailed elsewhere.[13,31] In general, AMBR is meant to describe a rotating magnetic bead system that rotates in an asynchronous fashion and can be used to monitor analytes. For the ferromagnetic system described here, the underlying behavior is as follows. When a magnetic particle is placed within an external rotating magnetic field, the average rotational frequency of the particle, $\langle\dot{\theta}\rangle$, is dependent on the driving field frequency, Ω. For magnetic particles with a permanent magnetic dipole, the external-field dependent rotational response of the bead is

$$\langle\dot{\theta}\rangle = 1/T = \begin{cases} \Omega & ; \quad \Omega<\Omega_c \\ \Omega - \sqrt{\Omega^2-\Omega_c^2} & ; \quad \Omega>\Omega_c \end{cases} ; \quad \Omega_c = mB/\eta V_{eff} \qquad [1]$$

Here Ω_c is the rotational critical frequency, m is the particle's magnetic moment, B is the magnetic field amplitude, η is the solution viscosity, and V_{eff} is the effective volume of the rotating body (which depends on both its volume and shape; for a spherical shape, it is 6 times the volume).[31] In order for the AMBR sensor to behave as a viscometer, the magnetic bead must be torqued at driving frequencies that are higher than the critical frequency; also, m, B, and V_{eff} must be held constant, such that the particle's rotational rate is solely dependent on the viscosity of the solution.[30,31] We also note that while the particle's rotation in this asynchronous regime is not in a steady-state, its *average* rotation frequency is well defined by equation [1]. The authors note that in principle, the described method will work with other types of magnetic beads, such as paramagnetic beads. For paramagnetic AMBR systems, the rotational period depends inversely on viscosity, namely $\langle\dot{\theta}\rangle \propto 1/\eta$.

3.2. AMBR viscometer characterization

The AMBR viscometer accurately measures temperature-dependent changes in the viscosity. To demonstrate this with the current system, a solution of PBS was heated from 34 – 46 °C, at 2 °C increments; increasing the solution temperature decreases suspension viscosity, which consequently decrease the bead's rotational period – see Equation [1] (Fig. 2a).

To validate these measurements, we calculated the viscosity of the PBS solutions at different temperature conditions using Eq. 1, given that the $m \sim 5.6 \times 10^{-16}$ Am^2, $B = 0.7$ mT, $V_{eff} = 3.14 \times 10^{-15}$ m^3 and from the bead's rotational rate. The viscosity of the solution can be determined from $\eta(T) = v_w(T)/\rho(T)$, where

$$\ln(v_w(T)) = 0.55908 - 0.03051T + 0.00015T^2,^{40} \qquad [2]$$

where $v_w(T)$ is the temperature-dependent viscosity and $\eta(T)$ is the temperature-dependent density of PBS. As shown in Figure 2(b), the viscosity measurements from AMBR agree with expected values that were calculated with Eq. 2. In addition, the AMBR sensor accurately measured the viscosity of various aqueous PBS-Glycerin solutions, at different glycerin concentrations, at a constant temperature (Fig. 2c). This agrees with what was reported in Ref 24. As a result, the AMBR viscometer was demonstrated to function

accurately as a viscometer within the viscosity range between 0.58 – 1.5 cP, which is sufficient to measure microbial growth within the experimental ranges described in this paper.

For use with bacteria, the AMBR particles must be passivated to eliminate the potential for bacterial binding to the particle. Particles functionalized with either carboxyl, amino, or streptavidin groups were incubated with the uropathogenic *E. coli* to determine the extent of non-specific binding. The magnetic particles that were functionalized with carboxyl-groups appeared to have little to no non-specific binding. In contrast, the amino- and streptavidin-functionalized magnetic particles had a large degree of non-specific binding to the particle surface (Supplementary Fig. 2). Nevertheless, non-specific binding may in fact improve platform sensitivity, as bacterial proliferation may result in both a viscosity and effective volume change of the particle, and thereby enhance the effect of bacterial growth on the particle's rotation.[13,14] However, to validate the AMBR as a bacterial viscometer, the carboxyl-functionalized magnetic particles were used.

3.3 Bacterial Growth

Individual AMBR viscometers that were suspended in an MH-PB bacteria solution were confined in nanoliter w/o (water/oil) droplets and the sensors were monitored with light microscopy. Within 20 minutes, there was a 20% increase in the AMBR sensor's rotational period for proliferating bacteria, i.e. growth and division, as compared to the non-proliferating bacteria (Fig. 3a,b). Bacterial growth resulted in an increase in the measured rotational period, which contrasted the steady rotational period value for bacteria treated with a lethal dose of sodium azide (NaN_3) (Fig. 3b). As the driving magnetic field and particle properties (magnetic moment, volume and shape) remained constant, we were able to isolate changes in rotational period to changes in the solution viscosity as bacteria proliferated [Eq. 1].

While planktonic growth was the primary mechanism acting to affect the rotational rate, other mechanisms may also affect the viscosity, including changes in the interfacial friction, increases in the absolute bacterial cell number, and protein secretion and accumulation during bacterial proliferation. Towards understanding and optimizing the AMBR viscometer, it was important to isolate the predominant factor affecting the bead's rotation. As the AMBR biosensor rests at the bottom of the droplet, near the aqueous/oil/glass interface, the magnetic particle experiences a frictional as well as a viscous resistive torque. The viscous torque of a sphere, T_s, is expressed by $T_s = (\frac{4\pi}{3})\beta R^3 \eta \Omega_s$, where β is a coefficient that is on the order of unity, R is the radius of the sphere, and Ω_s is the sphere's angular velocity.[41] The frictional torque, T_f, is expressed by $T_f = (\frac{8\pi}{9})\alpha\mu\Delta\rho g R^4$, where μ is the friction coefficient, $\Delta\rho$ is the difference between the densities of the sphere and the sample liquid, g is the gravity acceleration, and αR is the contact area between the sphere and the bottom of the cell.[41] Therefore, the total resistive torque on the AMBR system is,

$$T = T_s + T_f = (\tfrac{4\pi}{3})\beta R^3 \eta \Omega_s + (\tfrac{8\pi}{9})\alpha\mu\Delta\rho g R^4 \quad [2]$$

Considering that R is sufficiently small in our system, $R \sim 4 \times 10^{-6}$ to 9×10^{-6} m, the viscous force dominates the frictional torque, $T_s > T_f$. Furthermore, the viscous torque near the particle's equator dominates, as shown by

$$T(\theta)\, d\theta = 6\pi\eta R^3 \sin^3\theta d\theta, \quad 0 < \theta < \pi, \quad [3]$$

where $T(\theta)$ is the viscous torque at given regions of the particle, and $\theta = 0$ and $\theta = \pi$ at the bottom and top of the particle surface, respectively.[42] We thus demonstrate that both the frictional torque and the viscous torque near the outer regions of the hemispheres are negligible [Eq. 2 and 3] and that edge effects are not a major contributing factor to the changes in the bead's rotation. We examined this experimentally by repeating the experiment under different interfacial conditions, including using a different growth media, eliminating the oil phase, and removing the surfactant from the aqueous phase. Identical particle behavior was observed under all of these conditions [S.2]. We can, therefore, conclude that the change in the rotational response is caused by a change in the viscosity within the droplet.

The increase in the suspension viscosity upon bacterial proliferation may be a result from the accumulation of bacterial polysaccharides in the matrix, not from the absolute cell number (Fig. 3c). Bacteria are known to secrete bacterial polysaccharides, resulting in the broth developing viscoelastic, non-Newtonian characteristics,[24] which would lend itself to a slower rotational rate, as compared to Newtonian fluids.[46] The amount and type of bacterial polysaccharides secreted varies depending on the bacterial concentration and environmental conditions. As a result, the accumulation of polysaccharides and the transition to a viscoelastic suspension naturally increase the viscosity,[24] which subsequently translate to the increase in the particle's rotational period. While the accumulation of polysaccharides when cells proliferate may be one factor affecting the solution viscosity, the aim of this manuscript was to demonstrate the ability of the AMBR micro-viscometer to measure the viscosity of a bacterial system and to run AST and determine the MIC. As a result, confirmation of the presence of polysaccharides and viscosity independent environmental effects, such as pH changes or nutrient depletion, which arose from bacterial growth, was not studied in this manuscript, but will be studied in the future.

Even though bacterial growth resulted in viscosity increases, it was observed that at a unique time point, the AMBR viscometer's rotational period decreased, which would suggest an apparent decrease in the solution viscosity (Fig. 3b). The sudden drop in the rotational period may be explained by either biology or fluid dynamics. Possible explanations are that when bacteria grow to a significantly large population, bacteria motility changes, bacteria may excrete enzymes that break down the surrounding polysaccharide matrix, or the bacteria may incorporate polysaccharides from its surroundings.[17,24] Another possibility is that the rotating sensor may have generated a sufficient stress on the fluid, at which the viscoelastic behavior 'breaks down'. Nevertheless, this decrease in rotational period is consistent across various experimental conditions [Supplementary Fig. 3]. Experimental investigations to trend the rotational period with bacterial growth are ongoing.

3.4 Bacterial Response to Gentamicin

The AMBR viscometer was applied towards determining the gentamicin MIC of a uropathogenic strain of *E. coli*. The bacteria were cultured in 0, 0.25, 0.5, 1, and 2 μg/mL gentamicin concentrations and the rotational response and the corresponding viscosity changes of the suspension were monitored. The effects of gentamicin on bacterial proliferation could be discerned within 100 min, Figure 4. The rotational period for bacteria cultured in 0, 0.25, and 0.5 μg/mL gentamicin increased as the suspension's viscosity increased, thereby indicating bacterial growth. There was no observed change in the rotational period for bacteria cultured in solutions of 1 and 2 μg/mL gentamicin, which suggests that these are sufficiently high antibiotic concentrations for inhibition of bacterial growth. As demonstrated here, the AMBR viscometer, in its current state, is a tool that can measure the presence or lack of bacterial proliferation. Towards this end, we were unable to use the slope of the growth curve to indicate any quantitative information about the environmental condition or bacterial health. We presume that the different slopes of the

growth curves may result from slightly varying initial environmental and bacterial conditions that may affect the growth rate (Fig. 4 and Supplementary Fig. 3); however, further sensor and platform optimization and characterization need to be conducted to test this assumption. From the AMBR results shown in Figure 4, the gentamicin MIC was 1 μg/mL, which corresponds very well with the 1 μg/mL gentamicin MIC value of this strain, determined with the standard VITEK2 system.[14] When comparing MIC values of two methods, typically a two-fold dilution difference is acceptable.[10] A significant difference between the rotational responses of bacteria treated with the antibiotic above MIC conditions, versus below it, could be observed clearly, within 100 minutes. The authors suggest that this could be further reduced by measuring AMBR in a real-time manner and by applying more sophisticated algorithms, such as inflection point analysis.

4. Conclusion

We have demonstrated a label-free AMBR micro-viscometer that can measure the growth and drug susceptibility of a bacterial isolate more rapidly and using 1000-fold fewer initial bacteria counts than commercial phenotypic systems. We present proof-of-concept studies of the AMBR micro-viscometer towards measuring the gentamicin MIC of *E. coli* by measuring changes in the rheological properties of the bacterial suspension, comprised of an initial count of 50 bacteria. As bacteria proliferate, the viscosity of the solution increases, which translates to an increase in the magnetic bead's rotational period. This contrasts the constant rotational period that results from bacteria that are not proliferating, and hence do not change the solution viscosity. This label-free AST technique is extremely versatile, and therefore, can be easily extended for use on any planktonic bacteria strain without the need to develop specific antibodies.

Further developments of the system includes (1) increasing the throughput by monitoring a larger array of AMBR micro-viscometers consecutively and in real time, (2) using droplet sorting techniques to isolate droplets that contain AMBR micro-viscometers, and (3) integrating the system with an off-microscope sensor.[28,32] We anticipate that through parallelizing the platform and incorporating real-time data capture and analysis, the time to results for AST can be further reduced. In addition to microbial AST applications, we anticipate that the AMBR viscometer may be beneficial for measuring growth of any cell population, including prokaryotic and eukaryotic suspension cells, and for applications that require viscosity measurements of small samples, such as for biopolymer characterizations.[47]

Supplementary Material

Refer to Web version on PubMed Central for supplementary material.

Acknowledgments

This study was supported by NIH grant R21EB009550 (RK), NSF grant DMR 9900434 (RK), a Coulter grant (BHM/DN/RK), and the University of Michigan's Cellular Biotechnology Training Program (IS). The authors would also like to acknowledge Alex Hrin for creating the video capture LabVIEW program, Duane Newton, Ph.D., and John Younger, M.D., at the University of Michigan Medical School, for constructive discussions, the University of Michigan's (UM) Lurie Nanofabrication Facility (LNF), and the UM Chemical Engineering Clean Room for use of facilities, chemicals, and fabrication equipment.

References

1. Barenfanger J, Drake C, Kacich G. Clinical and Financial Benefits of Rapid Bacterial Identification and Antimicrobial Susceptibility Testing. J Clin Microbiol. 1999; 37:1415–1418. [PubMed: 10203497]

2. Chen CH, et al. Antimicrobial Susceptibility Testing Using High Surface-to-Volume Ratio Microchannels. Analytical Chemistry. 2010; 82:1012–1019. [PubMed: 20055494]
3. Martinez JL, et al. A global view of antibiotic resistance. FEMS Microbiology Reviews. 2009; 33:44–65. [PubMed: 19054120]
4. Costelloe C, Metcalfe C, Lovering A, Mant D, Hay AD. Effect of antibiotic prescribing in primary care on antimicrobial resistance in individual patients: systematic review and meta-analysis. BMJ. 2010; 340:c2096–c2096. [PubMed: 20483949]
5. Alvarez-Lerma F, et al. Empiric broad-spectrum antibiotic therapy of nosocomial pneumonia in the intensive care unit: a prospective observational study. Crit Care. 2006; 10:R78. [PubMed: 16704742]
6. Mach KE, et al. A Biosensor Platform for Rapid Antimicrobial Susceptibility Testing Directly From Clinical Samples. The Journal of Urology. 2011; 185:148–153. [PubMed: 21074208]
7. Jorgensen JH, Ferraro MJ. Antimicrobial Susceptibility Testing: General Principles and Contemporary Practices. Clinical Infectious Diseases. 1998; 26:973–980. [PubMed: 9564485]
8. Jorgensen JH, Ferraro MJ. Medical Microbiology: Antimicrobial Susceptibility Testing: A Review of General Principles and Contemporary Practices. Clinical Infectious Diseases. 2009; 49:1749–1755. [PubMed: 19857164]
9. Goldman, E.; Green, LH. Practical Handbook of Microbiology. CRC Press; 2008.
10. Health, C. for D. and R. Guidance Documents (Medical Devices and Radiation-Emitting Products) - Class II Special Controls Guidance Document: Antimicrobial Susceptibility Test (AST) Systems. at <http://www.fda.gov/MedicalDevices/DeviceRegulationandGuidance/GuidanceDocuments/ucm080564.htm>
11. Andrews JM. Determination of minimum inhibitory concentrations. Journal of Antimicrobial Chemotherapy. 2001; 48:5. [PubMed: 11420333]
12. Boedicker JQ, Li L, Kline TR, Ismagilov RF. Detecting bacteria and determining their susceptibility to antibiotics by stochastic confinement in nanoliter droplets using plug-based microfluidics. Lab Chip. 2008; 8:1265. [PubMed: 18651067]
13. Kinnunen P, et al. Monitoring the growth and drug susceptibility of individual bacteria using asynchronous magnetic bead rotation sensors. Biosensors and Bioelectronics. 2011; 26:2751–2755. [PubMed: 21095112]
14. Sinn I, et al. Asynchronous magnetic bead rotation (AMBR) biosensor in microfluidic droplets for rapid bacterial growth and susceptibility measurements. Lab Chip. 2011; 11:2604. [PubMed: 21666890]
15. Boedicker JQ, Vincent ME, Ismagilov RF. Microfluidic Confinement of Single Cells of Bacteria in Small Volumes Initiates High-Density Behavior of Quorum Sensing and Growth and Reveals Its Variability13. Angewandte Chemie. 2009; 121:6022–6025.
16. Ong KG, Wang J, Singh RS, Bachas LG, Grimes CA. Monitoring of bacteria growth using a wireless, remote query resonant-circuit sensor: application to environmental sensing. Biosensors and Bioelectronics. 2001; 16:305–312. [PubMed: 11390218]
17. Rafaï S, Jibuti L, Peyla P. Effective Viscosity of Microswimmer Suspensions. Phys Rev Lett. 2010; 104:098102. [PubMed: 20367014]
18. Stoyanov PG, Grimes CA. A remote query magnetostrictive viscosity sensor. Sensors and Actuators A: Physical. 2000; 80:8–14.
19. Sokolov A, Aranson IS. Reduction of Viscosity in Suspension of Swimming Bacteria. Phys Rev Lett. 2009; 103:148101. [PubMed: 19905604]
20. Cui Z. Weakly sheared active suspensions: hydrodynamics, stability, and rheology. Phys Rev E Stat Nonlin Soft Matter Phys. 2011; 83:031911. [PubMed: 21517529]
21. Hatwalne Y, Ramaswamy S, Rao M, Simha RA. Rheology of Active-Particle Suspensions. Phys Rev Lett. 2004; 92:118101. [PubMed: 15089176]
22. Saintillan D, Shelley MJ. Instabilities and pattern formation in active particle suspensions: kinetic theory and continuum simulations. Phys Rev Lett. 2008; 100:178103. [PubMed: 18518342]

23. Toda K, Furuse H, Amari T, Wei X. Cell concentration dependence of dynamic viscoelasticity of Escherichia coli culture suspensions. Journal of Fermentation and Bioengineering. 1998; 85:410–415.
24. Suresh Kumar A, Mody K, Jha B. Bacterial exopolysaccharides – a perception. Journal of Basic Microbiology. 2007; 47:103–117. [PubMed: 17440912]
25. Furuse H, Amari T, Miyawaki O, Asakura T, Toda K. Characteristic behavior of viscosity and viscoelasticity of Aureobasidium pullulans culture fluid. Journal of Bioscience and Bioengineering. 2002; 93:411–415. [PubMed: 16233223]
26. Sutherland IW. Biofilm exopolysaccharides: a strong and sticky framework. Microbiology. 2001; 147:3–9. [PubMed: 11160795]
27. Pang P, Cai Q, Yao S, Grimes CA. The detection of Mycobacterium tuberculosis in sputum sample based on a wireless magnetoelastic-sensing device. Talanta. 2008; 76:360–364. [PubMed: 18585290]
28. Kinnunen P, Sinn I, McNaughton BH, Kopelman R. High frequency asynchronous magnetic bead rotation for improved biosensors. Appl Phys Lett. 2010; 97:223701. [PubMed: 21200442]
29. McNaughton BH, Agayan RR, Clarke R, Smith RG, Kopelman R. Single bacterial cell detection with nonlinear rotational frequency shifts of driven magnetic microspheres. Appl Phys Lett. 2007; 91:224105.
30. McNaughton BH, Agayan RR, Wang JX, Kopelman R. Physiochemical microparticle sensors based on nonlinear magnetic oscillations. Sensors and Actuators B: Chemical. 2007; 121:330–340.
31. McNaughton BH, Kehbein KA, Anker JN, Kopelman R. Sudden Breakdown in Linear Response of a Rotationally Driven Magnetic Microparticle and Application to Physical and Chemical Microsensing. The Journal of Physical Chemistry B. 2006; 110:18958–18964. [PubMed: 16986890]
32. McNaughton BH, et al. Compact sensor for measuring nonlinear rotational dynamics of driven magnetic microspheres with biomedical applications. Journal of Magnetism and Magnetic Materials. 2009; 321:1648–1652.
33. Hecht A, Kinnunen P, McNaughton B, Kopelman R. Label-acquired magnetorotation for biosensing: An asynchronous rotation assay. Journal of Magnetism and Magnetic Materials. 2011; 323:272–278.
34. Hecht A, Kumar AA, Kopelman R. Label-Acquired Magnetorotation As a Signal Transduction Method for Protein Detection: Aptamer-Based Detection of Thrombin. Anal Chem. 2011; 83:7123–7128. [PubMed: 21805996]
35. Behrend, Anker J, McNaughton B, Kopelman R. Microrheology with modulated optical nanoprobes (MOONs). Journal of Magnetism and Magnetic Materials. 2005; 293:663–670.
36. Riesch C, Reichel EK, Keplinger F, Jakoby B. Characterizing Vibrating Cantilevers for Liquid Viscosity and Density Sensing. Journal of Sensors. 2008:697062.
37. Kuntner J, Stangl G, Jokoby B. Characterizing the rheological behavior of oil-based liquids: microacoustic sensors versus rotational viscometers. Sensors Journal, IEEE. 2005; 5:850–856.
38. Sanchez FG, Diaz AN, Ruiz CC, Guerrero MML. Fluid viscosity determination based on frequency domain time-resolved fluorescence anisotropy. Journal of Molecular Liquids. 2010; 155:121–126.
39. Pal R, et al. An integrated microfluidic device for influenza and other genetic analyses. Lab Chip. 2005; 5:1024–1032. [PubMed: 16175256]
40. Sinn I, et al. Magnetically uniform and tunable Janus particles. Appl Phys Lett. 2011; 98:024101.
41. McNaughton BH, et al. Fabrication of Nanoparticles and Microspheres with Uniform Magnetic Half-Shells. MRS Proceedings. 2006; 899E:988.
42. Anker JN, Kopelman R. Magnetically modulated optical nanoprobes. Appl Phys Lett. 2003; 82:1102.
43. Shankar PN, Kumar M. Experimental Determination of the Kinematic Viscosity of Glycerol-Water Mixtures. Proceedings of the Royal Society of London Series A: Mathematical and Physical Sciences. 1994; 444:573–581.
44. Sakai K, Hirano T, Hosoda M. Electromagnetically Spinning Sphere Viscometer. Applied Physics Express. 2010; 3:016602.

45. Hosoda M, Hirano T, Sakai K. Extension of Measurement Viscosity Range of EMS System. Proceedings of Symposium on Ultrasonic Electronics. 2010; 31:293–294.

46. D'Avino G, Cicale G, Hulsen MA, Greco F, Maffettone PL. Effects of confinement on the motion of a single sphere in a sheared viscoelastic liquid. Journal of Non-Newtonian Fluid Mechanics. 2009; 157:101–107.

47. Teyssandier F, Love BJ. MMA bulk polymerization and its influence on in situ resin viscosity comparing several chemorheological models. Journal of Applied Polymer Science. 2011; 120:1367–1371.

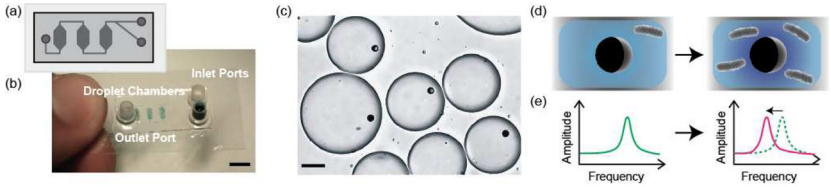

Figure 1.

AMBR micro-viscometer platform for cell proliferation studies. (a) Schematic and (b) assembled microfluidic droplet device. The chambers are filled with droplets dyed with blue food coloring. Scale bar: 5 mm (c) Light microscopy image of individual AMBR viscometers compartmentalized in nanoliter w/o microfluidic droplets. Scale bar: 50 μm. (d–e) Schematic of AMBR viscometer. (d) Bacterial growth in the surrounding solution changes the solution viscosity, which (e) shifts the particle's rotational frequency.

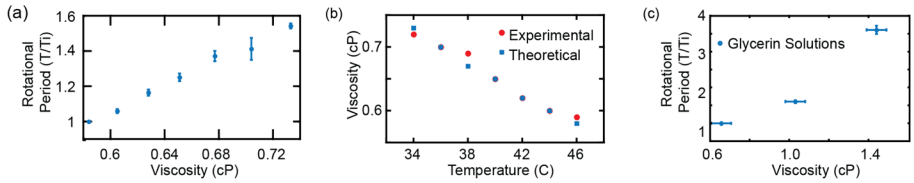

Figure 2.

AMBR micro-viscometer characterization. (a) Viscosity-dependent rotational response characterization of the AMBR viscometer sensor in the PBS buffer solution at different temperature values (34 to 46 °C). (b) The corresponding experimental and theoretical temperature-dependent viscosity values, as calculated with Eq. 2, at temperature values ranging from 34 to 46 °C in PBS solution. (c) Rotational response of the AMBR viscometer in glycerin solutions at different viscosities at 37 °C. Magnetically uniform Janus particles were used for all characterization experiments. The illustrated experimental error in the rotational period is the full width half max (FWHM) of the Fourier transform of the raw rotational signal.

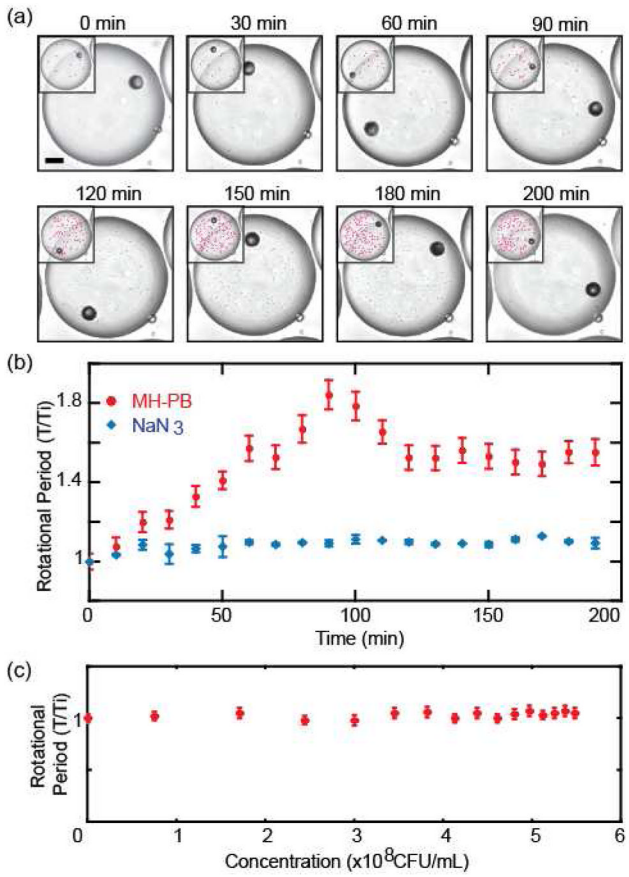

Figure 3.

Measuring growth-dependent viscosity changes using the AMBR micro-viscometer. (a) Light microscopy image of the AMBR viscometer system during bacterial growth in MH-PB growth medium. Scale-bar is 20 um. Inset: bacteria are highlighted in red to aid visualization. (b) Corresponding AMBR response curve for bacteria grown in MH-PB vs. a lethal dose of 0.5% Sodium Azide (NaN_3) in MH-PB. Bacterial growth is observed as an increase in the rotational period. There is no observed bacterial growth upon treatment with NaN_3, as indicated by “no change” in the rotational period. (c) Rotational response of the AMBR viscometer at different bacterial concentrations upon initial conditions (i.e. at time: 0 minutes). The steady rotational response suggests that the absolute number of bacteria in a given suspension does not affect the bead’s rotation, within the shown concentration range. The illustrated experimental error is equal to the standard deviation of measurement of the representative runs.

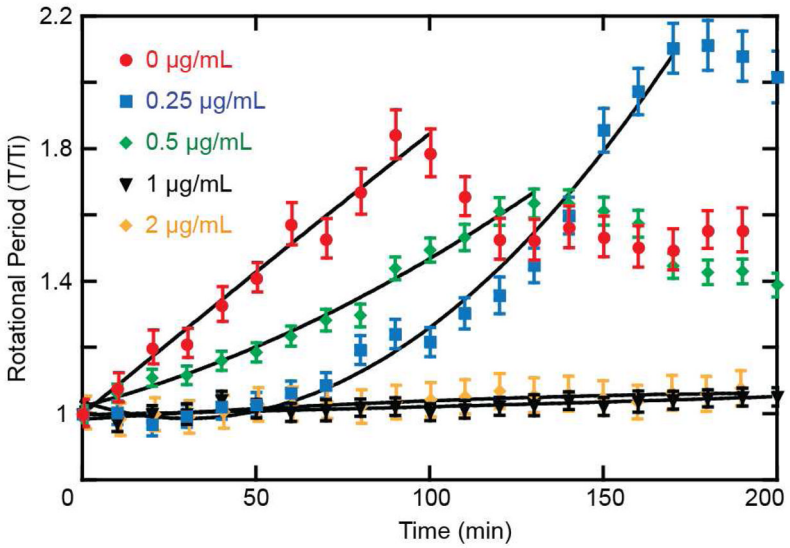

Figure 4.

Performing AST with the AMBR micro-viscometer. AMBR viscometer response to the proliferation of *E. coli* exposed to 0, 0.25, 0.5, 1, and 2 μg/mL gentamicin. An increase in the rotational period suggests bacterial growth/proliferation whereas a constant rotational period suggests growth inhibition. The data indicates an MIC of 1 μg/mL for gentamicin. The curve fits are provided to guide the eye. The illustrated experimental error is equal to the standard deviation of measurement of the representative runs.